Characterizing the mechanical properties of ectopic axonal receptive fields in inflamed nerves and following axonal transport disruption

Article (Accepted Version)

TITLE

Characterizing the mechanical properties of ectopic axonal receptive fields in inflamed nerves and following axonal transport disruption

AUTHORS

George Goodwin[A], Geoffrey M Bove[B], Bryony Dayment[A], Andrew Dilley[A]

AFFILIATION

[A] Brighton and Sussex Medical School, University of Sussex, Brighton BN1 9PS, UK

[B] University of New England, Biddeford, Maine, USA

CORRESPONDING AUTHOR:

Dr Andrew Dilley PhD
Department of Neuroscience,
Brighton and Sussex Medical School,
Medical Research Building,
University of Sussex,
Falmer,
Brighton BN1 9PS,
United Kingdom

Tel: +44 (0) 1273 877094
Fax: +44 (0) 1273 877884
Email: a.dilley@bsms.ac.uk

Disclosures: The authors would like to state that there are no conflicts of interest regarding this work.

Abstract

Radiating pain is a significant feature of chronic musculoskeletal pain conditions such as radiculopathies, repetitive motion disorders and whiplash associated disorders. It is reported to be caused by the development of mechanically-sensitive ectopic receptive fields along intact nociceptor axons at sites of peripheral neuroinflammation (neuritis). Since inflammation disrupts axonal transport, we have hypothesised that anterogradely-transported mechanically sensitive ion channels accumulate at the site of disruption, which leads to axonal mechanical sensitivity (AMS). In this study, we have characterised the mechanical properties of the ectopic axonal receptive fields and have examined the contribution of mechanically sensitive ion channels to the development of AMS following neuritis and vinblastine-induced axonal transport disruption. In both models, there was a positive force-discharge relationship and mechanical thresholds were low (~9 mN/mm^2). All responses were attenuated by ruthenium red and FM1-43, which block mechanically sensitive ion channels. In both models, the transport of TRPV1 and TRPA1 was disrupted, and intraneural injection of agonists of these channels caused responses in neurons with AMS following neuritis but not vinblastine treatment. In summary, these data support a role for mechanically sensitive ion channels in the development of AMS.

Keywords

Neuritis, neuroinflammation, axonal transport disruption, axonal mechanical sensitivity, transient receptor potential channels, nociceptors

Introduction

In chronic musculoskeletal pain conditions such as lumbar radiculopathies, repetitive motion disorders, whiplash associated disorders and carpal tunnel syndrome, tests that stretch nerve trunks (e.g. straight leg raise) or that apply pressure over nerve trunks (e.g. Tinel's sign) frequently cause radiating pain (Bove et al., 2005; Fernandez-de-Las-Penas et al., 2010; Greening et al., 2005; Ide et al., 2001; Sterling et al., 2002). On clinical examination, these patients rarely have signs of nerve or soft tissue injury that may account for symptoms. However, magnetic resonance imaging has demonstrated increases in nerve T2-signal in some of these patients that are consistent with neuritis (peripheral neuroinflammation) (Dilley et al., 2011; Greening et al., 2017). In a model of neuritis, intact through-conducting nociceptor axons develop ectopic receptive fields that are mechanical sensitivity to direct pressure and stretch at the inflamed site (Bove et al., 2003; Dilley and Bove, 2008; Dilley et al., 2005; Eliav et al., 2001; Satkeviciute et al., 2018). Therefore, we have hypothesised that inflammation-induced axonal mechanical sensitivity (AMS) underlies radiating pain in many patients with chronic musculoskeletal conditions (Bove and Dilley, 2019).

The cellular components necessary for mechanical transduction are conveyed from the soma to the peripheral terminals of primary sensory neurons by fast axonal transport (Koschorke et al., 1994). Since neuritis disrupts axonal transport (Dilley et al., 2013), we have proposed that transported mechanically sensitive ion channel components accumulate and become functional at the site of disruption, which leads to the development of an ectopic receptive field that responds to mechanical stimulation (Dilley and Bove, 2008). Consistent with this mechanism, the local disruption of axonal transport by vinca alkaloids, such as vinblastine, also leads to the development of AMS (Dilley and Bove, 2008).

The mechanically sensitive ion channels that contribute to the mechanism AMS have yet to be determined. Similarly, specific physiological characteristics of the ectopic axonal receptive fields have not been examined. Therefore, in the present study, we have examined the force-discharge relationships of C/slow Aδ-fibre axons with AMS following neuritis and local vinblastine treatment. As confirmation that AMS is due to activation of mechanically sensitive ion channels, we have examined the effects of ruthenium red and the styryl dye, FM1-43, on the force-discharge relationship. Both agents are reported to block mechanically sensitive ion channels in primary sensory neurons (Drew and Wood, 2007; Drew et al., 2002), which include members of the transient receptor potential family of channels (Fischer et al., 2003; Nagata et al., 2005; Qu et al., 2012; Quick et al., 2012; Voets et al., 2002), and piezo 1 and 2 (Coste et al., 2010; Coste et al., 2012; Eijkelkamp et al., 2013).

As part of this study, we have looked at the role of transient receptor potential vanilloid 1 (TRPV1) and ankyrin 1 (TRPA1) in the underlying mechanisms. Both channels are reported to mediate inflammation-induced mechanical sensitisation of nociceptors (Brederson et al., 2012; De Schepper et al., 2008; Kelly et al., 2015; Lennertz et al., 2012), and TRPA1 is considered to be in part responsible for noxious mechanical transduction (Brierley et al., 2011; Kerstein et al., 2009; Vilceanu and Stucky, 2010). Furthermore, there is also evidence that TRPV1 is transported by fast axonal transport (Biggs et al., 2007; Guo et al., 1999). Specifically, we have determined whether the transport of these channels is disrupted following neuritis and vinblastine-induced axonal transport disruption, and whether there is an increased functional presence of channels at the treatment site in nociceptor axons that are mechanically sensitive. In the latter experiments, the effects of N-oleoyldopamine (OLDA; a TRPV1 agonist (Chu et al., 2003)) and cinnamaldehyde (a TRPA1 agonist (Bandell et al., 2004)) on the activity rates of neurons with AMS were examined. Together, data from the present study have revealed the physiological characteristics of the ectopic axonal receptive fields and has demonstrated a role for mechanically sensitive ion channels.

Experimental procedures

Animals

Adult male Sprague Dawley rats (n = 87; Charles River, Kent, UK) were used in this study. Animals were housed in groups of two to four, in a 12/12 hour light/dark cycle, and were given ad libitum access to food and water. Experiments were carried out in strict accordance with the UK Animals (Scientific Procedures) Act (1986) and approval was also obtained from the University of Sussex Animal Welfare Ethical Review Board.

Surgeries

Neuritis was induced in 28 adult rats as previously described (Dilley and Bove, 2008). Under general anaesthesia (1.75% isoflurane-in oxygen), an incision was made through the skin on the posterolateral aspect of the thigh. The sciatic nerve was exposed by blunt dissection and a 7-8 mm length of nerve was carefully freed from the surrounding connective tissue. A strip of Gelfoam (5 × 5 × 10 mm, Spongostan™; Ferrosan, Denmark) saturated in 50% complete Freund's adjuvant (~150 µL; diluted in sterile 0.9% w/v saline) was loosely wrapped around the nerve. The muscle and skin were closed using 4/0 monofilament sutures (Vicryl; Ethicon, West London, United Kingdom) and the animals were allowed to recover.

Vinblastine was applied to the nerve of 25 rats as previously described (Dilley et al., 2013). The left sciatic nerve was exposed in the thigh by blunt dissection and a 7-8 mm length of nerve was freed from the surrounding connective tissue. A strip of parafilm (6 mm × 20 mm) was positioned under the nerve to prevent leakage of the drug onto the surrounding tissue. A strip of Gelfoam (5 × 5 × 10 mm) saturated in 0.1 mM vinblastine (~150 µL; diluted in 0.9% w/v saline) was loosely wrapped around the nerve. After 15 minutes, the Gelfoam and Parafilm were removed and the nerve was rinsed with saline. The muscle and skin were closed using 4/0 monofilament sutures.

The effects of neuritis, vinblastine and saline treatment on the anterograde transport of TRPV1 and TRPA1 were assessed by partially ligating the sciatic distal to the treatment site as previously described (Dilley et al., 2013). Briefly, a 7-8 mm length of nerve was freed from surrounding connective tissue, and 1/3-1/2 of the nerve was tightly ligated using 6-0 monofilament sutures (Vicryl; Ethicon). In one group of animals, a strip of gelfoam (5 x 5 x 10 mm) saturated in complete Freund's adjuvant was loosely wrapped around the nerve 2-4 mm proximal to the ligation (n = 6). In another group, a length of parafilm (6 x 20 mm) was positioned under the nerve, and a strip of Gelfoam saturated in either 0.1mM vinblastine (n =

8) or 0.9% w/v saline (n = 8) was loosely wrapped around the nerve 2-4 mm proximal to the ligation. After 15 min, the Parafilm and Gelfoam were removed from these animals and the nerve was rinsed with saline. The muscle and skin were closed using 4/0 monofilament sutures. Immunohistochemistry was used to compare the levels of TRPV1 and TRPA1 antibody immunofluorescence immediately proximal to the ligation.

Ex-vivo electrophysiology

Ex-vivo single-unit electrophysiological recordings from C/slow Aδ-fibre axons were carried out 3-8 days following neuritis (n = 94 neurons in 18 animals) and vinblastine treatment (n = 85 neurons in 10 animals) and in an additional untreated group (n = 89 neurons in 5 animals). Experiments were carried out using a custom recording chamber (Bove, 2011; Zimmermann et al., 2009). The chamber, which was constructed of thermoplastic (Delrin), consisted of two compartments: a larger main compartment, for superfusion of the nerve, and a smaller recording compartment (Fig. 1A). The compartments were separated by a 1 mm wall. Two 2 mm diameter apertures through the wall allowed exchange of perfusate between both compartments. A third aperture was used to pass the nerve through. The floor of the main compartment was lined with silicone (Sylgard 184 elastomer, Dow Corning, Midland, Michigan, USA), and a groove within the silicone supported the nerve. Synthetic interstitial fluid (SIF (Bretag, 1969)), bubbled with 95% oxygen/5% carbon dioxide, was flowed into the main compartment of the chamber, the level of which could be adjusted using a sluice. A one metre vertical column maintained the hydrostatic pressure of the SIF, and the flow rate of the SIF was regulated through a drip chamber (1 drop/sec; Alaris, Becton Dickinson, San Diego, California, USA). The temperature of the SIF was monitored using a thermistor (TH10K, Thor Labs, Newton, New Jersey, USA) mounted within the wall of the main compartment. A foil resistive heater (HT10K, Thor Labs) within the floor of the chamber was used to warm the SIF to 32 ˚C, which was controlled with a temperature controller (TC200, Thor Labs). A raised glass platform (9 x 5 mm) within the recording compartment supported the proximal end of the nerve. The recording compartment was topped up with mineral oil above the level of the glass platform. The level of the SIF was adjusted using the sluice so that it was just below the height of the glass platform.

Animals were overdosed with sodium pentobarbital (200 mg/kg, intraperitoneally) and transcardially perfused with SIF containing heparin. The left sciatic nerve and its L5 anterior primary ramus were carefully dissected from the L5 intervertebral foramen to the popliteal fossa, and transferred into the main compartment of the chamber. The proximal end of the nerve was passed through the aperture from the main compartment into the recording

compartment using a curved 30-gauge needle, where it was placed onto the glass platform. Within the main compartment, the nerve was pinned by its connective tissue with fine insect pins into the groove on the silicone floor. The nerve was incubated for one hour in the chamber prior to recording.

Bipolar stimulating electrodes were used to stimulate the nerve. The anode, which was a shielded tungsten needle electrode (World Precision Instruments, Sarasota, Florida, USA), was positioned in the nerve distal to the treatment site so that the unshielded tip was in contact with the nerve. For proximal stimulation, or stimulation at the treatment site, the electrode was positioned in the connective tissue surrounding the nerve. The cathode, a platinum wire electrode, was located within the SIF close to the distal portion of the nerve. A ground electrode was positioned under the nerve within the main compartment.

Individual fine filaments were teased from the L5 anterior primary ramus (~6-10 μm in diameter) using finely sharpened forceps and placed over gold bipolar recording electrodes. Electrical stimulation (square-wave pulses; 0.5 ms duration, 2-20 V amplitude) was applied using a constant-voltage isolated stimulator (Digitimer, Hertfordshire, United Kingdom). Only clearly identifiable waveforms were studied (<15 C/slow Aδ-fibre waveforms per filament). The number of C/slow Aδ-fibres on each filament was determined by slowly increasing the stimulus amplitude until the maximum number of waveforms was elicited. Action potentials were amplified (1-5 K), band-pass filtered (10-5,000 Hz) and monitored with an oscilloscope, and digitised using Spike 2 software (Cambridge Electronic Designs, Cambridge, United Kingdom). Neurons were classified based on waveform shape and conduction velocity, which was determined from the conduction distance and latency of individual waveforms. Conduction velocities below 1.5 m/s were considered C/slow Aδ-fibres (Harper and Lawson, 1985).

Axonal mechanical sensitivity testing

The nerve was initially searched for mechanically sensitive ectopic axonal receptive fields using a tapered silicone probe as previously described (Bove et al., 2003). Once a mechanically sensitive axon was identified, its conduction velocity was determined by electrically stimulating the nerve while mechanically stimulating the ectopic axonal receptive field. If the axon fired in response to mechanical stimulation immediately prior to the electrical stimulation of the nerve, the same axon evoked by the electrical stimulus would be delayed or would not be initiated (i.e. the electrical stimulus occurred during the refractory period). Following identification of a mechanically sensitive C/slow Aδ-fibre axon, a

feedback-controlled mechanical stimulator (modified 300C-LR, Aurora Scientific, Aurora, Ontario, Canada) was used to apply increasing forces to the nerve. The arm of the stimulator was fitted with a 2 mm^2 silicone tip, which was lowered onto the ectopic axonal receptive field using a micromanipulator. The initial resting force of the probe on the nerve was below the level that caused activation of the axon. The mechanical stimulator was controlled using Spike 2 software. During mechanical testing, forces were applied as a series of six incremental, 2 sec, 25mN steps from 25 to 175 mN above the initial resting force. There was 1 sec interval between each step. Prior to drug application, the step protocol was repeated three times at two-minute intervals. Following drug application (see below), the step protocol was repeated five times.

Application of blockers of mechanosensitive ion channels

Following identification of a mechanically sensitive axon, a brass ring (8 mm diameter), which was notched to accommodate the nerve, was positioned over the nerve at the ectopic axonal receptive field and sealed around its base using petroleum jelly. The height of the ring was greater than the depth of the surrounding fluid, so that when filled, a positive pressure would be present thus maintaining the concentration of the test fluid. Initially, the well was topped up with SIF. After baseline mechanical sensitivity testing, the SIF within the well was replaced with increasing concentrations of ruthenium red (R2751; 10-50 μM; Sigma-Aldrich, Gillingham, UK) or FM1-43 (T3163, 2.5-25 μM, Thermo Fisher Scientific, Waltham, MA, USA), which were diluted in SIF. Final concentrations of both agents were made up on the day of the experiment from 10mM aliquots that had been stored at -20°C. The concentrations examined were based on those previously shown to block mechanically-activated currents in primary sensory neurons (Drew and Wood, 2007; Di Castro et al., 2006). Each concentration of drug was applied for a total of 20 minutes. After 10 minutes of drug application, the mechanical stimulation protocol was repeated five times at two-minute intervals (Fig. 2A). All treatment groups underwent the same blocker application protocol except for two vinblastine-treated nerves where an additional concentration of 10 μM FM1-43 was applied. Electrical stimulation of the nerve, as well as AMS testing with the tapered probe, were used to confirm that the nerve was still conducting following drug application. In preliminary experiments, SIF was applied to the AMS receptive fields (n = 3) to determine whether repeated mechanical testing effected the firing frequency produced at 150 mN force, the slope of the force-discharge response or the firing threshold.

In vivo electrophysiology

In vivo single-unit electrophysiological recordings from C/slow Aδ-fibre axons in the L5 dorsal root were carried out 3-8 days following neuritis (n = 88 neurons in 13 animals) and vinblastine treatment (n = 83 neurons in 12 animals) as previously described (Bove et al., 2003). An additional group of experiments was carried out on untreated animals (n = 55 neurons in 7 animals). Animals were anesthetized with 1.5 g/kg 25% w/v urethane intraperitoneally and the body temperature was maintained at 37°C using a rectal thermistor probe connected to a heated pad (Harvard Apparatus, Kent, United Kingdom). A lumbar laminectomy was performed from L2 to L5 to expose the spinal canal. The surrounding skin was sutured to a metal ring to form a pool filled with warmed mineral oil. The dura mater was opened and the left L5 dorsal root was cut close to the spinal cord. The cut end of the dorsal root was placed onto a glass platform (9 × 5 mm). In the thigh, the sciatic nerve was exposed at the treatment site, or equivalent nerve segment in untreated animals, and a plastic platform (9 x 5 mm) that was notched to support the nerve was positioned under the nerve.

Fine filaments were teased from the cut end of the dorsal root and individually placed onto paired gold recording electrodes. Bipolar stimulating electrodes positioned under the L5 dorsal root were used to electrically stimulate the nerve (square wave pulses: 0.5–0.9 ms duration and 10–30 V amplitude) using a constant-voltage isolated stimulator. The electrical stimulus was increased so that the maximum number of waveforms was elicited (<7 C/slow Aδ-fibre waveforms on each filament). Action potentials were amplified (1-5 K) and band-passed filtered (10-5,000 Hz), and digitised using Spike 2 software.

Cutaneous and deep receptive fields for isolated neurons were searched below the knee. Most receptive fields were located by squeezing the periphery, using either fingers or forceps. The loose property of the skin was exploited to carefully discriminate cutaneous versus deep fields (Bove et al., 2003). Cutaneous neurons had receptive fields that remained associated with the skin regardless of the skin excursion. In contrast, deep neurons were identified by moving the skin and repeating the effective stimulus to the same underlying spot. Following receptive field identification, the conduction velocity of the neuron was determined by electrically stimulating the dorsal root while mechanically stimulating the receptive field. If the neuron fired to mechanically-evoked stimulation of the receptive field immediately prior to the electrical stimulation of the nerve, the same neuron evoked by the electrical stimulus would be delayed or would not be initiated. Since neurons with AMS generally innervate deep structures (Bove et al., 2003; Dilley and Bove, 2008; Satkeviciute et al., 2018), receptive fields with deep locations were preferentially searched in untreated

animals. Following receptive field characterization, the neuron was tested at the treatment site for AMS using the tapered silicone probe described above. After a neuron with AMS had been identified, its conduction velocity was determined by electrically stimulating the dorsal root while mechanically stimulating the treatment site. Spike shape and conduction velocity were used to confirm that the neuron with the characterized receptive field and the neuron that had AMS were the same.

Agonist application

To avoid leakage of agents onto the surrounding soft tissues, a strip of Parafilm was positioned below the treatment site (or equivalent length of nerve in untreated animals). Both OLDA (1641, Tocris, Abingdon, Oxford, UK) and cinnamaldehyde (W228613, Sigma-Aldrich) were diluted in 1% Dimethyl sulfoxide/0.5% ethanol in SIF (vehicle). Final concentrations of both agents were made up on the day of the experiment from aliquots (1mM OLDA; 10mM cinnamaldehyde) that had been stored at -20°C. The concentrations of OLDA and cinnamaldehyde examined were based on those previously shown to activate TRPV1 (Chu et al., 2003; Gavva et al., 2004) and TRPA1 respectively (Bandell et al., 2004; Nassenstein et al., 2008). Initially, following a 5 min exposure to vehicle, ascending concentrations of OLDA (10, 50 and 200 μM) and cinnamaldehyde (100, 250 and 500 μM) were topically applied to the treatment site for 10 min each using gelfoam (5 × 5 × 10 mm) saturated in the drug (~200 μl). However, the topical application of agonists had negligible effect on activity levels (refer to Supplementary Material), and therefore the nerve was copiously washed with SIF, after which 100μL of vehicle, 50 μM OLDA, or 500 μM cinnamaldehyde were intraneurally injected at the treatment site using a 30-gauge needle, bent to a 45° angle. These concentrations were selected based upon that of previous studies (Chu et al., 2003; Gavva et al., 2004) (Bandell et al., 2004; Nassenstein et al., 2008). All drugs were made from stock solutions on the day of the experiment and warmed to 37 ˚C before application. Ongoing activity levels were assessed 2 min immediately prior to injection, and for up to 10 min post-injection. Receptive fields and AMS were re-tested for each neuron following the 10 min post-injection period to ensure that the injection did not cause damage to the axon.

Immunohistochemistry

On day four postoperative, neuritis (n = 6), vinblastine-treated (n = 8), and saline-treated rats (n = 8) were overdosed with sodium pentobarbital (200 mg/kg, intraperitoneally), and the left sciatic nerve at the ligation site removed. Nerve segments (~10 mm length) were snap frozen in isopentane on dry ice and stored at -80 ˚C overnight. Longitudinal 16 μm sections

were cut using a cryostat (Leica Microsystems, Wetzlar, Germany) and thaw-mounted on gelatin-coated glass slides. Sections were blocked with 4% normal goat serum (Vector Labs, Burlingame, USA) in phosphate-buffered saline (PBS) (Sigma, UK) for 1 hour at room temperature and incubated overnight at 4 ˚C with polyclonal rabbit anti-TRPV1 (NB100-1617; Novus Biologicals, Abingdon, United Kingdom; diluted 1:500 in 4% normal goat serum in PBS) or anti-TRPA1 primary antibodies (ACC-03, Alomone Labs, Jerusalem, Israel; diluted 1:300 in 4% normal goat serum in PBS). Both antibodies have been previously tested in rat and mouse tissue (Liapi and Wood, 2005; Sharif Naeini et al., 2006; Stein et al., 2006; Sullivan et al., 2015; Yamamoto et al., 2015). Sections were incubated in the dark for one hour at room temperature with Alexa Fluro 488 goat anti-rabbit (Thermo Fisher Scientific, Loughborough, United Kingdom; diluted 1:200 in PBS), followed by fixation for 7 minutes in 4% paraformaldehyde (in PBS). Slides were dried and cover-slipped using glycerol/PBS mounting medium (Citifluor, London, UK). Between steps, sections were washed 3 times for 10 minutes in PBS. Slides were viewed under a fluorescence microscope (Leica Microsystems) at 488-nm excitation and photographed. Non-specific staining with secondary antibody was not found in the absence of primary antibody in any case.

Analysis

Data were tested for normality using Shapiro-Wilk tests. For analysis of the electrophysiology data, conduction velocities were compared between models using Kruskal-Wallis tests followed by Dunn's post hoc tests. The frequency of firing evoked by 150 mN force and the slope of the force-discharge response, which is given as Hz/mN, were compared between models using Student's t tests, whereas and mechanical threshold was compared using Mann Whitney tests. The effects of FM1 -43 and ruthenium red on the number of spikes in response to 150 mN force, slope of the force-discharge response and the percent change of each of these parameters were compared between models using two-way analysis of variance (ANOVA). The mean activity rate pre- and post- the intraneural injection of vehicle, OLDA and cinnamaldehyde were also compared for each model using two-way ANOVA. The p values are given for the main effect, unless stated. The mean rate post-intraneural injection was calculated from the 2 min bin with the highest rate change for each individual experiment. For analysis of the immunohistochemistry data, images of the ligation site were converted to greyscale using Image J software. A region of interested was drawn over the ligated portion of the nerve that extended from the ligation site, 200 μm proximally (Govea et al., 2017). A region of interest was also drawn over the adjacent unligated portion of nerve that also extended 200 μm proximally. Care was taken to avoid

blood vessels, which stained positive for both TRPV1 and TRPA1. The median grayscale value was determined for each region of interest, and a ratio was calculated by dividing the median intensity of the ligated axons by the median intensity of the axons in the unligated portion of the nerve. Mean ratios were compared between models using one-way ANOVA. Post hoc analyses were conducted using Fisher's least significant- difference test, correcting for the false discovery rate as per Benjamini and Hochberg (Benjamini and Hochberg, 1995). Data are presented as mean +/- standard error of the mean (SEM).

Results

Ex-vivo force-discharge responses

The median conduction velocity of the through-conducting C/slow Aδ-fibre axons was 0.68 m/s (IQR = 0.18) in the untreated group (n = 89 neurons) and 0.69 m/s (IQR = 0.16) in the neuritis group (n = 57 neurons). Following vinblastine treatment, the median conduction velocity (0.61 m/s (IQR = 0.16); n = 85 neurons) was significantly reduced compared to the untreated and neuritis groups ($p < 0.001$, Kruskal-Wallis). Positioning of the simulating electrodes either side of the treatment site revealed conduction block in 76% (n =37/49 neurons in 5 experiments) of C/slow Aδ-fibre axons at the inflammatory site. There was no indication of a similar conduction blocked following vinblastine treatment.

Ectopic receptive fields that responded to direct mechanical stimulation were present along C/slow Aδ-fibre axons following neuritis and vinblastine treatment, and were confined to single discrete locations at, or immediately proximal to (1-2 mm), the treatment site. Similar ectopic receptive fields were not found along C/slow Aδ-fibre axons in the untreated group (n = 89 neurons examined). Only axons with mechanical sensitivity where the mechanical stimulator could be positioned reliably over the receptive field were examined. Typical responses to mechanical stimulation of the receptive field with increasing force (~25-175 mN) are shown in Fig. 1B. Following neuritis and vinblastine treatment, mechanical stimulation of the receptive field with incremental mechanical force resulted in a clear positive force-discharge response in the majority of neurons, i.e. as the force increased, the firing response also increased (Fig. 1B). For one axon following neuritis, the increasing force did not cause an increase in responses (* on Fig. 1E). All of the axons with mechanical sensitivity conducted through the treatment site, except for one axon following neuritis that could not be stimulated electrically distal to the inflammatory site. However, the ectopic axonal receptive field was proximal to the stimulating site. Responses to repeat trials (n= 3) were similar (e.g. Fig. 1C, D). The mean coefficient of determination (r^2) for regression lines fitted to the repeat trial data was 0.48 (0.1 SEM) and 0.58 (0.05 SEM) following neuritis and vinblastine treatment respectively. The mean firing frequency produced at 150 mN force, slope of the force-discharge relationship and mechanical threshold are shown in table 1. The slope of the force-discharge response and the mechanical threshold were significantly greater following vinblastine treatment compared to the neuritis group ($p<0.05$).

Effects of mechanically sensitive ion channel blockers on force-discharge responses

During ex vivo experiments, either FM1-43 or ruthenium red were applied to ectopic receptive fields on C/slow Aδ-fibre neurons following neuritis and vinblastine treatment. Vehicle was also applied to ectopic axonal receptive fields following vinblastine treatment to confirm that repeated mechanical stimulation does not affect the firing frequency produced at 150 mN force, the slope of the force-discharge response or the firing threshold (Table 2). Typical responses to mechanical stimulation following the application of FM1-43 and ruthenium red are shown in Figure 2B-E.

In both models, FM1-43 caused a dose-dependent decrease in the rate of firing evoked by 150mN force ($F(2, 10) = 11.03$, $p < 0.01$, two-way ANOVA, Fig. 2F; percent change, Fig. 2J). FM1-43 also caused a decrease in the slope of the force-discharge response in the vinblastine-treated group but not following neuritis ($F(2, 10) = 5.15$ [interaction], $p < 0.05$, Fig. 2G; percent change, Fig. 2K). Similar to FM1-43, ruthenium red caused a dose-dependent decrease in the rate of firing evoked by 150mN force in both models ($F(3, 18) = 6.29$, $p < 0.05$, Fig. 2H; percent change, Fig. 2L), as well as slope of the force discharge response ($F(3, 18) = 5.07$, $p < 0.05$, Fig. 2I; percent change, Fig. 2M). The application of FM1-43 and ruthenium red had negligible effect on the mechanical threshold of the ectopic axonal receptive fields following neuritis or vinblastine treatment (Table 3). With the exception of the single neuron where conduction across the treatment site could not be determined, electrical stimulation of the nerve distal to the treatment site following the application of FM1-43 and ruthenium red confirmed that neither agent blocked conduction.

Responses to intraneural injection of TRPV1 and TRPA1 agonists

In vivo recordings were made from 88 C/slow Aδ-fibre neurons following neuritis, of which 17 were mechanically sensitive at the treatment site, and 83 C/slow Aδ-fibre neurons following vinblastine treatment, of which 12 were mechanically sensitive at the treatment site. In both groups, ectopic axonal receptive fields were located at, or immediately proximal to, the treatment site. All of the neurons with AMS had receptive fields within deep tissues in the leg or at the ankle joint that responded to firm pressure. Receptive fields were not characterised for neurons without AMS. Recordings were also made from 55 C/slow Aδ-fibre neurons in untreated animals, of which receptive fields in deep structures in the leg and ankle were identified in 11 of these neurons. None of the neurons in the untreated group had AMS. The median conduction velocities were 0.39 m/s (IQR = 0.18), 0.42 m/s (IQR = 0.22) and 0.47 m/s (IQR = 0.26) in the neuritis, vinblastine-treated and untreated groups respectively. The

proportion of neurons that had ongoing activity at baseline was 27.3% (24/88) following neuritis (median rate = 0.06 Hz (IQR = 0.19)), 14.4% (12/83) following vinblastine treatment (median rate = 0.04 Hz (IQR = 0.32)) and 12.7% (7/55) in the untreated group (median rate = 0.02 Hz (IQR = 0.15)).

In the neuritis and vinblastine-treated groups, OLDA, cinnamaldehyde or vehicle were injected into the treatment site. For the neurons in the neuritis group with ectopic axonal receptive fields, there was a significant transient increase in activity within 10 min following the intraneural injection of OLDA and cinnamaldehyde compared to baseline (F (1, 14) = 9.95, p<0.01, two-way ANOVA; Fig. 3A-E). All of the responses peaked within two minutes following cinnamaldehyde injection (Fig. 3D). For those neurons in the neuritis group without ectopic axonal receptive fields, there was no significant increase in activity following the injection of OLDA or cinnamaldehyde (F (1, 68) = 3.43, p = 0.068; table 4). In the vinblastine-treated group, neither OLDA nor cinnamaldehyde caused an increase in activity in neurons with ectopic axonal receptive fields (F (1, 8) = 1.27, p = 0.29; Fig. 3F-H) or those without (F (1, 64) = 0.37, p = 0.54; table 4). The intraneural injection of OLDA or cinnamaldehyde into the untreated group had negligible effects on activity levels during the 10 min recording period (F (1, 8) = 3.39, p = 0.10; table 4).

Evidence for disruption of TRPV1 and TRPA1 transport

Following saline treatment, there was clear immunolabeling of TRPV1 immediately proximal to the ligation on day 4 postoperative, whereas there was negligible immunolabeling in adjacent unligated nerve. In contrast, immunolabeling of TRPV1 was decreased immediately proximal to the ligation site in the vinblastine-treated and neuritis groups (F (2, 10) = 4.78, p < 0.05, one-way ANOVA. Fig. 4A, B). A similar pattern of immunolabeling was observed for TRPA1 (F (2, 8) = 5.57, p < 0.05, one-way ANOVA; Fig. 4C, D). For both channels, the decrease in immunolabeling was most apparent following vinblastine treatment.

Discussion

Mechanical sensitivity along intact nociceptor axons is considered to underlie movement-evoked radiating pain. In this study, we compared the mechanical properties of axons at sites of neuritis to those treated with vinblastine, the latter of which disrupts axonal transport in the absence of inflammation. The present data has added to our previous studies on the role of neuritis as the cause of mechanical sensitivity. Specifically, we have shown that the majority of mechanically sensitive axons have a clear, positive force-discharge relationship, and that the forces necessary to activate these axons are low. We have shown that AMS is reduced following the application of the mechanically sensitive ion channel blockers, ruthenium red and FM1-43. Finally, we have revealed a potential role for TRPV1 and TRPA1 in the underlying mechanisms.

There is no information on the transduction properties of inflamed mechanically sensitive through-conducting axons. It should be emphasized that untreated axons do not normally respond to mechanical stimuli (Bove et al., 2003; Dilley and Bove, 2008; Dilley et al., 2005). The graded responses reported in this study are comparable to mechanical responses at the peripheral terminals of nociceptors, which also show a positive force-discharge relationship (Banik and Brennan, 2008; Garell et al., 1996; Handwerker et al., 1987; Khalsa et al., 1997; Koltzenburg et al., 1997). Since we have previously proposed that mechanically sensitive channels destined for the terminals accumulate at the site of disruption, it is possible that similar mechanisms underlie the transduction of mechanical stimuli at both sites. As such, following neuritis and vinblastine treatment, the axon membrane at the treatment site behaves as a remote extension of the peripheral terminal. The majority of cutaneous C-fiber terminals are polymodal (Bessou and Perl, 1969). Since a recent study has shown this characteristic along nociceptive axons following neuritis (noxious mechanical and chemical stimuli) (Govea et al., 2017), it seems likely that the axon membranes of some neurons in this study would have responded to other noxious stimuli. Limitations in the method prevented us from including multiple stimuli.

The steeper response slopes following vinblastine treatment suggest that ectopic axonal receptive fields are more responsive in this model compared to neuritis. This correlates with a more pronounced axonal transport disruption following vinblastine treatment (Dilley et al., 2013). The difference in responsiveness could also reflect the thickened epi-perineurium and granuloma that occur due to neuritis (Bove et al., 2003; Bove et al., 2009; Eliav et al., 1999; Bove et al., 2019), neither of which develop following vinblastine treatment (Dilley and Bove, 2008). In both models, the mechanical thresholds were relatively low, which is consistent with a previous study (Bove and Light, 1995). Correcting for probe size (2 mm^2), neurons

responded to pressures of approximately 9 mN/mm^2 following neuritis and vinblastine treatment, which is comparable to those forces that activate regenerating sprouts at a neuroma (Rivera et al., 2000) and injured muscle C-fibre afferents (Tode et al 2018). These values are less than the pressure that is reported to evoke painful responses over nerve trunks in patients with carpal tunnel syndrome and whiplash associated disorder (approximately 200 mN/mm^2) (Fernandez-de-las-Penas et al., 2009; Scott et al., 2005), but in our study the forces are applied directly on the nerve rather than through varying thicknesses of skin and other soft tissues. The findings further support a role for inflammation-induced AMS in nociceptors as the cause of nerve trunk mechanical sensitivity in these patients.

The dose-dependent decrease in the firing rate at 150 mN force following the local application of FM1-43 and ruthenium red supports that mechanically sensitive ion channels, such as transient receptor potential and piezo channels, which have also been implicated in mechanical transduction at the peripheral terminals (Sexton et al., 2016; Woo et al., 2015), may underlie inflammatory- and vinblastine-induced AMS. This result was further confirmed by the observed decrease in the slope of the force-discharge response following drug application (i.e. the agents reduced the responsiveness of the ectopic axonal receptive fields), and the tendency for the threshold of the response to increase. However, these agents are not specific to mechanically sensitive channels. For example, ruthenium red has been shown to block other channels, such as voltage-gated calcium channels and two-pore-domain potassium channels (Cibulsky et al., 1999; Braun et al., 2015). The local inhibition of channels that are not mechanically sensitive may alter membrane excitability, which could impact the frequency of action potential firing during AMS testing. The activity of both ruthenium red and FM1-43 were most apparent on axons in vinblastine treated nerves, which could be due to the thickened epi-perineurium of inflamed nerves presenting more of a barrier for the drugs to gain access to the axons. Preliminary experiments, where SIF was applied within the ring, confirmed that the observed drug effects were not simply due to repeated mechanical testing. Furthermore, control experiments confirmed that the effects were not due to conduction block.

Although the majority of ex-vivo recordings were from axons that conducted through the treatment site, there was a notable block of conduction at the inflammatory site that was not evident following vinblastine treatment or during in vivo studies (Dilley et al., 2005). Such conduction block may reflect a reduction in available oxygen and other metabolites, which ex-vivo rely on penetration through the greatly thickened epi-perineurium (Bove and Barbe 2009).

Increased labelling of TRPV1 and TRPA1 immediately proximal to the ligation site in saline-treated nerves confirmed that both channels are transported by fast anterograde transport. Furthermore, a decrease in labelling at the ligation site following neuritis and vinblastine treatment is consistent with the disruption of this process in both models, and the subsequent accumulation of these channels at the site of disruption. From this data, however, it is not possible to determine the density of channel accumulation at the treatment sites and how this compares to the receptive fields. Since both models are short-term, the accumulation may only be modest. A transient increase in firing from C/slow Aδ-fibre neurons following the intraneural injection of TRPV1 and TRPA1 agonists at the neuroinflammatory site confirmed that, as well as being present, both ion channels were functional at this location. Since the responses to both OLDA and cinnamaldehyde were confined to neurons with AMS, we have hypothesised that TRPV1 and TRPA1 may contribute to axonal excitability, and possibly mechanical sensitivity, in this subgroup of neurons, which is consistent with their role in inflammation-induced mechanical sensitisation of nociceptors (Brederson et al., 2012; De Schepper et al., 2008; Kelly et al., 2015), and noxious mechanical transduction (Brierley et al., 2011; Kerstein et al., 2009; Vilceanu and Stucky, 2010). In contrast, there was an absence of response to both OLDA and cinnamaldehyde injection at the vinblastine treatment site, which suggests that TRPV1 and TRPA1 are unlikely to underlie AMS in this model. Although the transport of both channels is disrupted, there may be fewer inserted into the axon membrane, which is consistent with the reports that inflammatory mediators increase the insertion of TRP channels (Camprubi-Robles et al., 2009; Meng et al., 2016; Stein et al., 2006; Zhang et al., 2005).

In summary, inflammation- and vinblastine-induced ectopic axonal receptive fields are characterized by graded responses that are attenuated by agents that act on mechanically sensitive ion channels, such as TRP channels. As such, the present data support our previously proposed mechanism whereby mechanically sensitive ion channels accumulate at, or just proximal to, the site of disruption, which leads to a mechanically sensitive receptive field on the nerve. Our data have revealed small differences in the mechanical properties of axons between models, which suggest that inflammation may play a role in defining the characteristics of the mechanical responses following neuritis. For example, local inflammation may influence the insertion, expression, or sensitisation of the accumulating channels. The current findings add to our understanding of the mechanisms of radiating pain, which is a feature of a diverse, although seemingly related, group of conditions that include lumbar radiculopathies, repetitive motion disorders, whiplash associated disorders, carpal tunnel syndrome as well as fibromyalgia and complex regional pain syndrome.

References:

Bandell M, Story GM, Hwang SW, Viswanath V, Eid SR, Petrus MJ, Earley TJ, Patapoutian A (2004) Noxious cold ion channel TRPA1 is activated by pungent compounds and bradykinin. Neuron 41:849-857.

Banik RK, Brennan TJ (2008) Sensitization of primary afferents to mechanical and heat stimuli after incision in a novel in vitro mouse glabrous skin-nerve preparation. Pain 138:380-391.

Benjamini Y, Hochberg Y (1995) Controlling the False Discovery Rate - a Practical and Powerful Approach to Multiple Testing. J Roy Stat Soc B Met 57:289-300.

Bessou P, Perl ER (1969) Response of cutaneous sensory units with unmyelinated fibers to noxious stimuli. J Neurophysiol 32:1025-1043.

Biggs JE, Yates JM, Loescher AR, Clayton NM, Boissonade FM, Robinson PP (2007) Vanilloid receptor 1 (TRPV1) expression in lingual nerve neuromas from patients with or without symptoms of burning pain. Brain Res 1127:59-65.

Bove GM, Vinblastine applied to sciatic nerve induces ectopic endogenous chemical sensitivities of slowly conducting axons, ex-vivo., Society for Neuroscience, Washington, DC, 2011.

Bove GM, Delany SP, Hobson L, Cruz GE, Harris MY, Amin M, Chapelle SL, Barbe MF (2019) Manual therapy prevents onset of nociceptor activity, sensorimotor dysfunction, and neural fibrosis induced by a volitional repetitive task. Pain 160:632-644.

Bove GM, Dilley A (2019) A lesson from classic British literature. Lancet 393:1297-1298.

Bove GM, Light AR (1995) Unmyelinated nociceptors of rat paraspinal tissues. J Neurophysiol 73:1752-1762.

Bove GM, Ransil BJ, Lin HC, Leem JG (2003) Inflammation induces ectopic mechanical sensitivity in axons of nociceptors innervating deep tissues. J Neurophysiol 90:1949-1955.

Bove GM, Weissner W, Barbe MF (2009) Long lasting recruitment of immune cells and altered epi-perineurial thickness in focal nerve inflammation induced by complete Freund's adjuvant. J Neuroimmunol 213:26-30.

Bove GM, Zaheen A, Bajwa ZH (2005) Subjective nature of lower limb radicular pain. J Manipulative Physiol Ther 28:12-14.

Braun G, Lengyel M, Enyedi P, Czirják G (2015) Differential sensitivity of TREK-1, TREK-2 and TRAAK background potassium channels to the polycationic dye ruthenium red. Br J Pharmacol 172:1728-1738.

Brederson JD, Chu KL, Reilly RM, Brown BS, Kym PR, Jarvis MF, McGaraughty S (2012) TRPV1 antagonist, A-889425, inhibits mechanotransmission in a subclass of rat primary afferent neurons following peripheral inflammation. Synapse 66:187-195.

Bretag AH (1969) Synthetic interstitial fluid for isolated mammalian tissue. Life Sci 8:319-329.

Brierley SM, Castro J, Harrington AM, Hughes PA, Page AJ, Rychkov GY, Blackshaw LA (2011) TRPA1 contributes to specific mechanically activated currents and sensory neuron mechanical hypersensitivity. J Physiol 589:3575-3593.

Camprubi-Robles M, Planells-Cases R, Ferrer-Montiel A (2009) Differential contribution of SNARE-dependent exocytosis to inflammatory potentiation of TRPV1 in nociceptors. FASEB J 23:3722-3733.

Chu CJ, Huang SM, De Petrocellis L, Bisogno T, Ewing SA, Miller JD, Zipkin RE, Daddario N, et al. (2003) N-oleoyldopamine, a novel endogenous capsaicin-like lipid that produces hyperalgesia. J Biol Chem 278:13633-13639.

Cibulsky SM, Sather WA (1999) Block by ruthenium red of cloned neuronal voltage-gated calcium channels. J Pharmacol Exp Ther 289:1447-1453.

Coste B, Mathur J, Schmidt M, Earley TJ, Ranade S, Petrus MJ, Dubin AE, Patapoutian A (2010) Piezo1 and Piezo2 are essential components of distinct mechanically activated cation channels. Science 330:55-60.

Coste B, Xiao B, Santos JS, Syeda R, Grandl J, Spencer KS, Kim SE, Schmidt M, et al. (2012) Piezo proteins are pore-forming subunits of mechanically activated channels. Nature 483:176-181.

De Schepper HU, De Winter BY, Van Nassauw L, Timmermans JP, Herman AG, Pelckmans PA, De Man JG (2008) TRPV1 receptors on unmyelinated C-fibres mediate colitis-induced sensitization of pelvic afferent nerve fibres in rats. J Physiol 586:5247-5258.

Di Castro A, Drew LJ, Wood JN, Cesare P (2006) Modulation of sensory neuron mechanotransduction by PKC- and nerve growth factor-dependent pathways. Proc Natl Acad Sci U S A 103:4699-4704.Dilley A, Bove GM (2008) Disruption of axoplasmic transport induces mechanical sensitivity in intact rat C-fibre nociceptor axons. J Physiol 586:593-604.

Dilley A, Bove GM (2008) Resolution of inflammation-induced axonal mechanical sensitivity and conduction slowing in C-fiber nociceptors. J Pain 9:185-192.

Dilley A, Greening J, Walker-Bone K, Good C (2011) Magnetic resonance imaging signal hyperintensity of neural tissues in diffuse chronic pain syndromes: a pilot study. Muscle Nerve 44:981-984.

Dilley A, Lynn B, Pang SJ (2005) Pressure and stretch mechanosensitivity of peripheral nerve fibres following local inflammation of the nerve trunk. Pain 117:462-472.

Dilley A, Richards N, Pulman KG, Bove GM (2013) Disruption of fast axonal transport in the rat induces behavioral changes consistent with neuropathic pain. J Pain 14:1437-1449.

Drew LJ, Wood JN (2007) FM1-43 is a permeant blocker of mechanosensitive ion channels in sensory neurons and inhibits behavioural responses to mechanical stimuli. Mol Pain 3:1.

Drew LJ, Wood JN, Cesare P (2002) Distinct mechanosensitive properties of capsaicin-sensitive and -insensitive sensory neurons. J Neurosci 22:RC228.

Eijkelkamp N, Linley JE, Torres JM, Bee L, Dickenson AH, Gringhuis M, Minett MS, Hong GS, et al. (2013) A role for Piezo2 in EPAC1-dependent mechanical allodynia. Nat Commun 4:1682.

Eliav E, Benoliel R, Tal M (2001) Inflammation with no axonal damage of the rat saphenous nerve trunk induces ectopic discharge and mechanosensitivity in myelinated axons. Neurosci Lett 311:49-52.

Eliav E, Herzberg U, Ruda MA, Bennett GJ (1999) Neuropathic pain from an experimental neuritis of the rat sciatic nerve. Pain 83:169-182.

Fernandez-de-las-Penas C, de la Llave-Rincon AI, Fernandez-Carnero J, Cuadrado ML, Arendt-Nielsen L, Pareja JA (2009) Bilateral widespread mechanical pain sensitivity in carpal tunnel syndrome: evidence of central processing in unilateral neuropathy. Brain 132:1472-1479.

Fernandez-de-Las-Penas C, Ortega-Santiago R, Ambite-Quesada S, Jimenez-Garci AR, Arroyo-Morales M, Cleland JA (2010) Specific mechanical pain hypersensitivity over peripheral nerve trunks in women with either unilateral epicondylalgia or carpal tunnel syndrome. J Orthop Sports Phys Ther 40:751-760.

Fischer MJ, Reeh PW, Sauer SK (2003) Proton-induced calcitonin gene-related peptide release from rat sciatic nerve axons, in vitro, involving TRPV1. Eur J Neurosci 18:803-810.

Garell PC, McGillis SLB, Greenspan JD (1996) The mechanical response properties of nociceptors innervating feline hairy skin. J Neurophysiol 75:1177-89.

Gavva NR, Klionsky L, Qu Y, Shi L, Tamir R, Edenson S, Zhang TJ, Viswanadhan VN, et al. (2004) Molecular determinants of vanilloid sensitivity in TRPV1. J Biol Chem 279:20283-20295.

Govea RM, Barbe MF, Bove GM (2017) Group IV nociceptors develop axonal chemical sensitivity during neuritis and following treatment of the sciatic nerve with vinblastine. J Neurophysiol 118:2103-2109.

Greening J, Anantharaman K, Young R, Dilley A (2018) Evidence for increased MRI signal intensity and morphological changes in the brachial plexus and median nerves of patients with chronic arm and neck pain following whiplash injury. J Orthop Sports Phys Ther 48:523-532.

Greening J, Dilley A, Lynn B (2005) In vivo study of nerve movement and mechanosensitivity of the median nerve in whiplash and non-specific arm pain patients. Pain 115:248-253.

Guo A, Vulchanova L, Wang J, Li X, Elde R (1999) Immunocytochemical localization of the vanilloid receptor 1 (VR1): relationship to neuropeptides, the P2X(3) purinoceptor and IB4 binding sites. Eur J Neurosci 11:946-958.

Handwerker HO, Anton F, Reeh PW (1987) Discharge patterns of afferent cutaneous nerve fibers from the rat's tail during prolonged noxious mechanical stimulation. Exp Brain Res 65:493-504.

Harper AA, Lawson SN (1985) Electrical properties of rat dorsal root ganglion neurones with different peripheral nerve conduction velocities. J Physiol 359:47-63.

Ide M, Ide J, Yamaga M, Takagi K (2001) Symptoms and signs of irritation of the brachial plexus in whiplash injuries. J Bone Joint Surg Br 83:226-229.

Kelly S, Chapman RJ, Woodhams S, Sagar DR, Turner J, Burston JJ, Bullock C, Paton K, et al. (2015) Increased function of pronociceptive TRPV1 at the level of the joint in a rat model of osteoarthritis pain. Ann Rheum Dis 74:252-259.

Kerstein PC, del Camino D, Moran MM, Stucky CL (2009) Pharmacological blockade of TRPA1 inhibits mechanical firing in nociceptors. Mol Pain 5:19.

Khalsa PS, LaMotte RH, Grigg P (1997) Tensile and compressive responses of nociceptors in rat hairy skin. J Neurophysiol 78:492-505.

Koltzenburg M, Stucky CL, Lewin GR (1997) Receptive properties of mouse sensory neurons innervating hairy skin. J Neurophysiol 78:1841-1850.

Koschorke GM, Meyer RA, Campbell JN (1994) Cellular components necessary for mechanoelectrical transduction are conveyed to primary afferent terminals by fast axonal transport. Brain Res 641:99-104.

Lennertz RC, Kossyreva EA, Smith AK, Stucky CL (2012) TRPA1 mediates mechanical sensitization in nociceptors during inflammation. PLoS One 7:e43597.

Liapi A, Wood JN (2005) Extensive co-localization and heteromultimer formation of the vanilloid receptor-like protein TRPV2 and the capsaicin receptor TRPV1 in the adult rat cerebral cortex. Eur J Neurosci 22:825-834.

Meng J, Wang J, Steinhoff M, Dolly JO (2016) TNFalpha induces co-trafficking of TRPV1/TRPA1 in VAMP1-containing vesicles to the plasmalemma via Munc18-1/syntaxin1/SNAP-25 mediated fusion. Sci Rep 6:21226.

Nagata K, Duggan A, Kumar G, Garcia-Anoveros J (2005) Nociceptor and hair cell transducer properties of TRPA1, a channel for pain and hearing. J Neurosci 25:4052-4061.

Nassenstein C, Kwong K, Taylor-Clark T, Kollarik M, Macglashan DM, Braun A, Undem BJ (2008) Expression and function of the ion channel TRPA1 in vagal afferent nerves innervating mouse lungs. J Physiol 586:1595-1604.

Qu L, Li Y, Pan X, Zhang P, LaMotte RH, Ma C (2012) Transient receptor potential canonical 3 (TRPC3) is required for IgG immune complex-induced excitation of the rat dorsal root ganglion neurons. J Neurosci 32:9554-9562.

Quick K, Zhao J, Eijkelkamp N, Linley JE, Rugiero F, Cox JJ, Raouf R, Gringhuis M, et al. (2012) TRPC3 and TRPC6 are essential for normal mechanotransduction in subsets of sensory neurons and cochlear hair cells. Open Biol 2:120068.

Rivera L, Gallar J, Pozo MA, Belmonte C (2000) Responses of nerve fibres of the rat saphenous nerve neuroma to mechanical and chemical stimulation: an in vitro study. J Physiol 527 Pt 2:305-313.

Satkeviciute I, Goodwin G, Bove GM, Dilley A (2018) The time course of ongoing activity during neuritis and following axonal transport disruption. J Neurophysiol 119:1993-2000.

Scott D, Jull G, Sterling M (2005) Widespread sensory hypersensitivity is a feature of chronic whiplash-associated disorder but not chronic idiopathic neck pain. Clin J Pain 21:175-181.

Sexton JE, Desmonds T, Quick K, Taylor R, Abramowitz J, Forge A, Kros CJ, Birnbaumer L, et al. (2016) The contribution of TRPC1, TRPC3, TRPC5 and TRPC6 to touch and hearing. Neurosci Lett 610:36-42.

Sharif Naeini R, Witty MF, Seguela P, Bourque CW (2006) An N-terminal variant of Trpv1 channel is required for osmosensory transduction. Nat Neurosci 9:93-98.

Stein AT, Ufret-Vincenty CA, Hua L, Santana LF, Gordon SE (2006) Phosphoinositide 3-kinase binds to TRPV1 and mediates NGF-stimulated TRPV1 trafficking to the plasma membrane. J Gen Physiol 128:509-522.

Sterling M, Treleaven J, Jull G (2002) Responses to a clinical test of mechanical provocation of nerve tissue in whiplash associated disorder. Man Ther 7:89-94.

Sullivan MN, Gonzales AL, Pires PW, Bruhl A, Leo MD, Li W, Oulidi A, Boop FA, et al. (2015) Localized TRPA1 channel Ca2+ signals stimulated by reactive oxygen species promote cerebral artery dilation. Sci Signal 8:ra2.

Tode J, Kirillova-Woytke I, Rausch VH, Baron R, Janig W (2018) Mechano- and thermosensitivity of injured muscle afferents 20 to 80 days after nerve injury. J Neurophysiol 119:1889-901.

Vilceanu D, Stucky CL (2010) TRPA1 mediates mechanical currents in the plasma membrane of mouse sensory neurons. PLoS One 5:e12177.

Voets T, Prenen J, Vriens J, Watanabe H, Janssens A, Wissenbach U, Bodding M, Droogmans G, et al. (2002) Molecular determinants of permeation through the cation channel TRPV4. J Biol Chem 277:33704-33710.

Woo SH, Lukacs V, de Nooij JC, Zaytseva D, Criddle CR, Francisco A, Jessell TM, Wilkinson KA, et al. (2015) Piezo2 is the principal mechanotransduction channel for proprioception. Nat Neurosci 18:1756-1762.

Yamamoto K, Chiba N, Chiba T, Kambe T, Abe K, Kawakami K, Utsunomiya I, Taguchi K (2015) Transient receptor potential ankyrin 1 that is induced in dorsal root ganglion neurons contributes to acute cold hypersensitivity after oxaliplatin administration. Mol Pain 11:69.

Zhang X, Huang J, McNaughton PA (2005) NGF rapidly increases membrane expression of TRPV1 heat-gated ion channels. Embo J 24:4211-4223.

Zimmermann K, Hein A, Hager U, Kaczmarek JS, Turnquist BP, Clapham DE, Reeh PW (2009) Phenotyping sensory nerve endings in vitro in the mouse. Nat Protoc 4:174-196.

Table 1. Ectopic axonal receptive field characteristics.

	Neuritis group	Vinblastine-treated group	p
Firing frequency at 150 mN force (Hz), mean (SEM)	5.60 (1.21)	7.10 (1.17)	0.38*
Slope (Hz/mN), mean (SEM)	0.027 (0.008)	0.055 (0.007)	<0.01*
Mechanical threshold (mN), median (IQR)	34.8 (3.06)	38.3 (27.9)	<0.05†

* Student t test. † Mann Whitney test.

Table 2. Effects of vehicle application on repeated mechanical testing of ectopic receptive fields (See Fig. 2A for protocol).

	Baseline	Final repeat testing	% change	p
Firing frequency at 150 mN force (Hz), mean (SEM)	5.84 (1.58)	5.92 (1.80)	2.18% (14.8%)	0.94*
Slope (Hz/mN), mean (SEM)	0.071 (0.016)	0.070 (0.017)	-1.64% (19.1%)	0.92*
Mechanical threshold (mN), median (IQR)	79.72 (30.15)	79.72 (30.15)	0% (0%)	1†

n = 3 vinblastine-treated animals. * Student t test. † Mann Whitney test.

Table 3. Effects of FM1-43 and ruthenium red on the mechanical threshold of ectopic receptive fields.

		Threshold (mN), mean (SEM)	
Blocker	**Model**	**Pre-**	**Post-**
FM1-43	Neuritis	32.02 (1.23)	32.02 (1.23)
	Vinblastine	36.28 (1.29)	36.28 (1.29)
Ruthenium red	Neuritis	48.54 (7.66)	55.19 (13.33)
	vinblastine	46.76 (6.63)	53.40 (13.06)

Post- represents the mechanical threshold following the application of the highest dose of each agent (25μM FM1-43 and 50 μM ruthenium red). n = 4 neurons in each group, except neurons following neuritis that were tested with FM1-43 (n = 3).

Table 4. Mean activity rates of neurons without ectopic axonal receptive fields.

			Activity rate (Hz), mean (SEM)	
Model	**Agent**	**n**	**Pre-**	**Post-**
Neuritis	Vehicle	27	0.002 (0.052)	0.004 (0.084)
	OLDA	14	0.027 (0.018)	0.033 (0.019)
	Cinnamaldehyde	30	0.056 (0.025)	0.089 (0.039)
Vinblastine treatment	Vehicle	20	0.000 (0.000)	0.000 (0.000)
	OLDA	22	0.006 (0.004)	0.002 (0.002)
	Cinnamaldehyde	25	0.053 (0.026)	0.067 (0.033)
Untreated	OLDA	5†	0.005 (0.003)	0.015 (0.010)
	Cinnamaldehyde	5†	0.022 (0.018)	0.028 (0.021)

Post-activity rate represents the two min bin post-injection with the highest mean rate. † Peripheral receptive fields characterised.

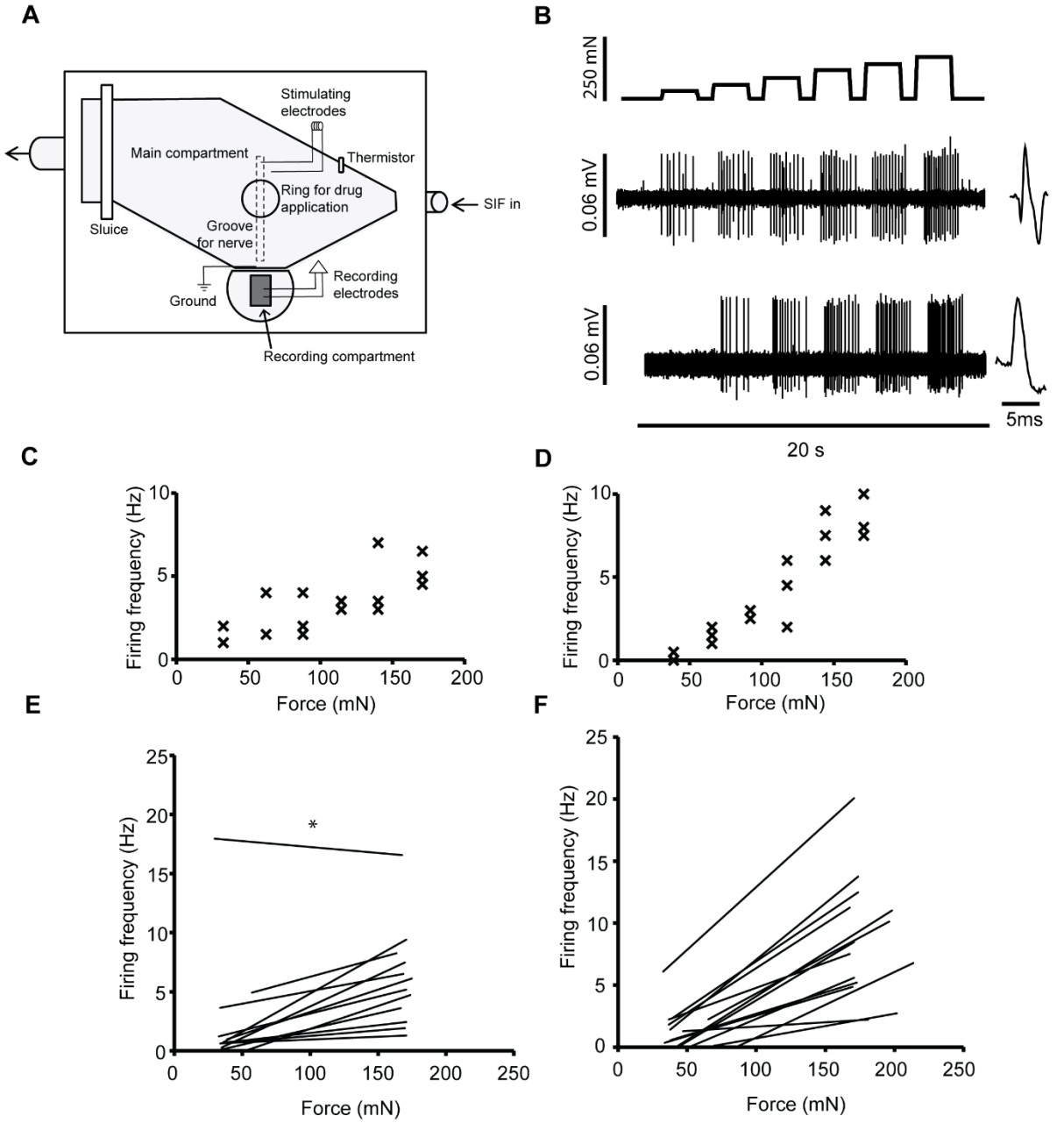

Fig. 1. Force-discharge responses in ex-vivo experiments. (A) Schematic diagram of the ex-vivo electrophysiology apparatus. (B) Typical force-discharge responses following neuritis (middle trace) and vinblastine treatment (lower trace). Forces were applied to each ectopic axonal receptive field as a series of six incremental, 2 sec, steps from 25 mN to 175 mN above the initial resting force (i.e. the force of the probe against the nerve; upper trace). (C, D) Typical examples of the force-discharge responses following (C) neuritis and (D) vinblastine treatment. Each graph represents three repeat trials. (E, F) Regression lines for individual ectopic axonal receptive fields in (E) neuritis and (F) vinblastine-treated animals. n = 12 and 14 AMS neurons respectively. * AMS neuron with plateaued force-discharge response.

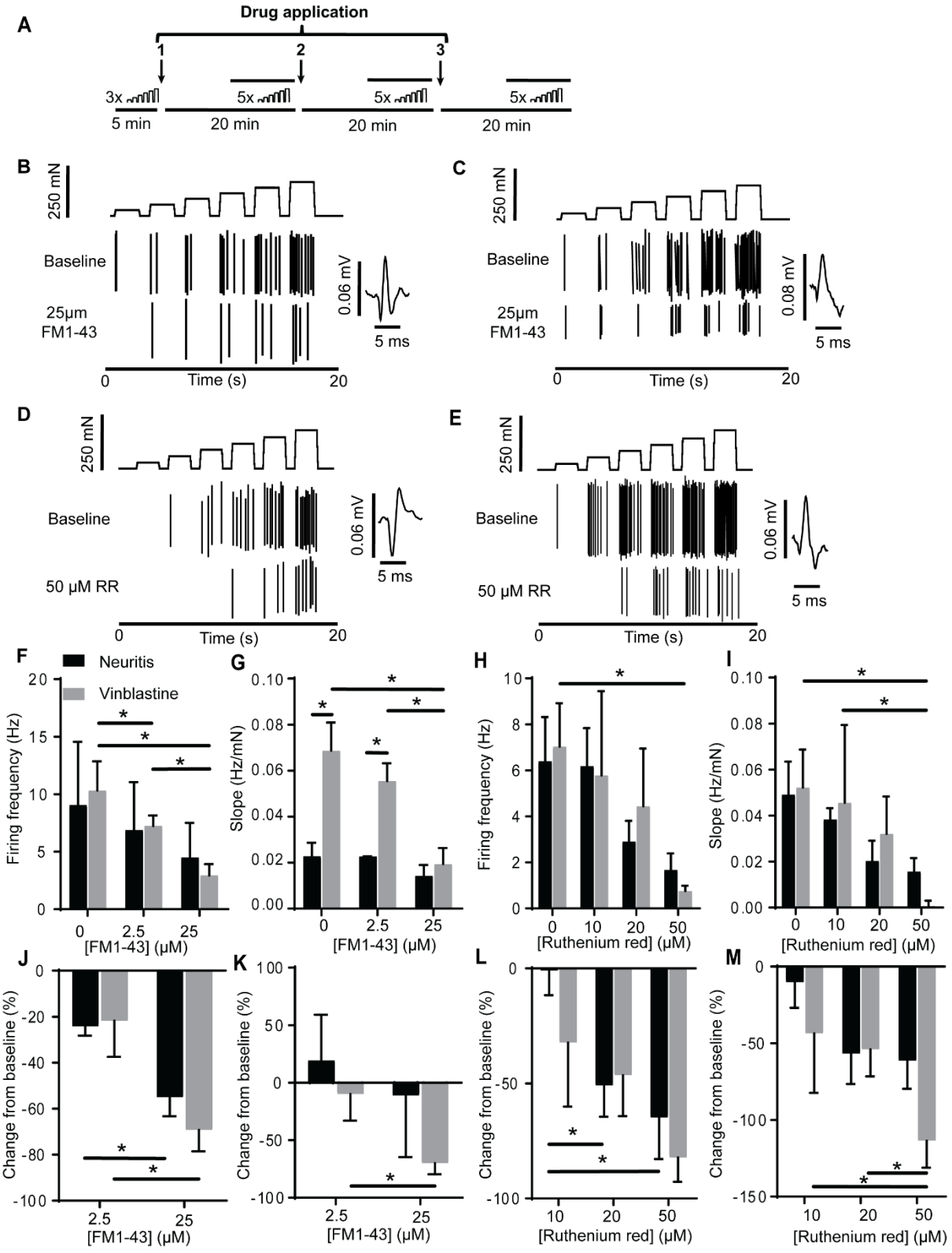

Fig. 2. Application of blockers of mechanically sensitive ion channels to ectopic axonal receptive fields. (A) Experimental design (refer to methods). (B-E) Typical responses following 25 µM FM1-43 and 50 µM ruthenium red (RR) application to ectopic axonal

receptive fields following (B, D) neuritis and (C, E) vinblastine treatment. (F, G) The mean firing frequency produced at 150mN force and (H, I) slope of the force discharge relationship following the application of FM1-43 or ruthenium red. (J, K) The mean percent change from baseline in the firing frequency at 150mN force and (H, I) slope of the force discharge relationship following the application of FM1-43 or ruthenium red. * $p<0.05$ (two-way ANOVA followed by Fisher's least significant-difference post hoc test, correcting for the false discovery rate). In G, the interaction was significant ($p <0.05$). n = 4 neurons in each group, except neurons following neuritis that were tested with FM1-43 (n = 3). Error bars = SEM.

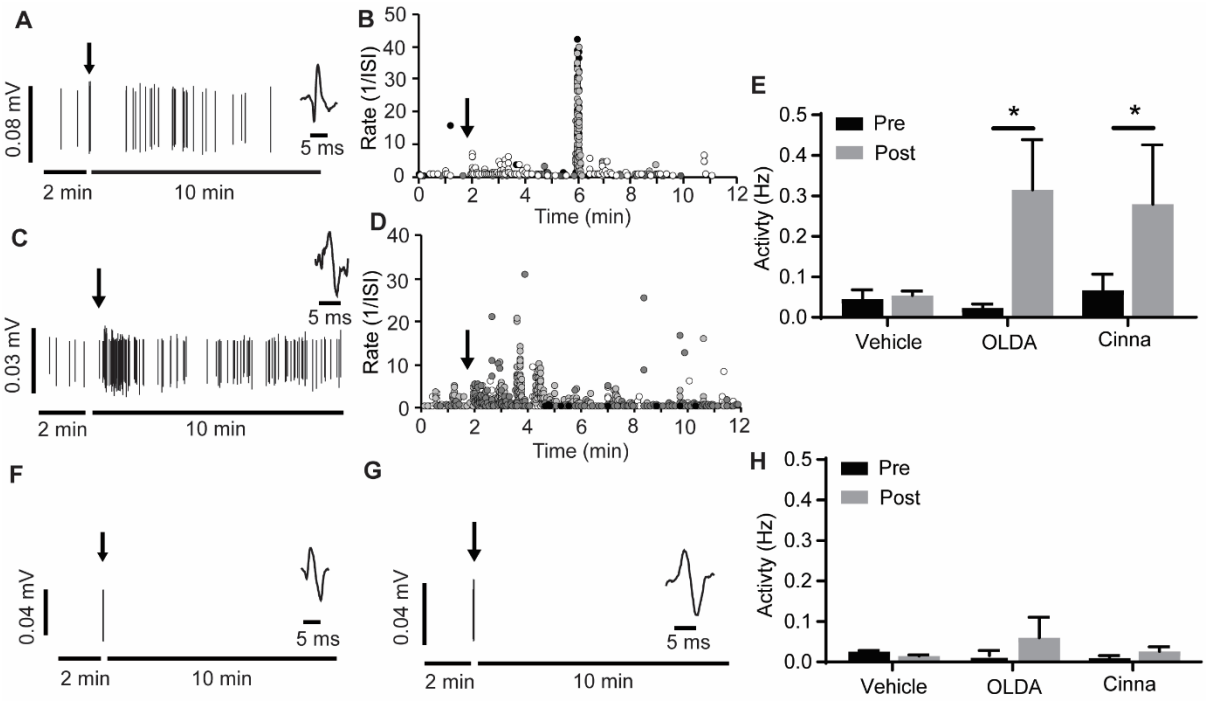

Fig. 3. Responses of C/slow Aδ-fibre neurons with ectopic receptive fields to the intraneural injection of vehicle, 50 μM N-oleoyl-dopamine (OLDA) and 500 μM cinnamaldehyde.(A, C) Typical responses following injection of (A) OLDA and (C) cinnamaldehyde into the inflammatory site. (B, D) Activity rates of individual neurons during the 10 min recording period following the intraneural injection of (B) OLDA and (D) cinnamaldehyde into the inflammatory site. (E) Mean activity levels pre- and post- the intraneural injection of vehicle, OLDA or cinnamaldehyde into the inflammatory site. The mean post-intraneural injection was calculated from the 2 min bin with the maximum firing rate for each neuron. (F, G) Typical responses following injection of (F) OLDA and (G) cinnamaldehyde into the vinblastine treatment site. (H) Mean activity levels pre- and post- the intraneural injection of vehicle, OLDA or cinnamaldehyde into the vinblastine treatment site. * $p<0.05$ (two-way ANOVA followed by Fisher's least significant-difference post hoc test, correcting for the false discovery rate). For neuritis: n = 5, 6 and 6 neurons, exposed to OLDA, cinnamaldehyde and vehicle respectively. For vinblastine treatment: n = 4, 4 and 3 neurons, exposed to OLDA, cinnamaldehyde and vehicle respectively. Arrows indicate drug application. ISI, Interspike interval. Error bars = SEM.

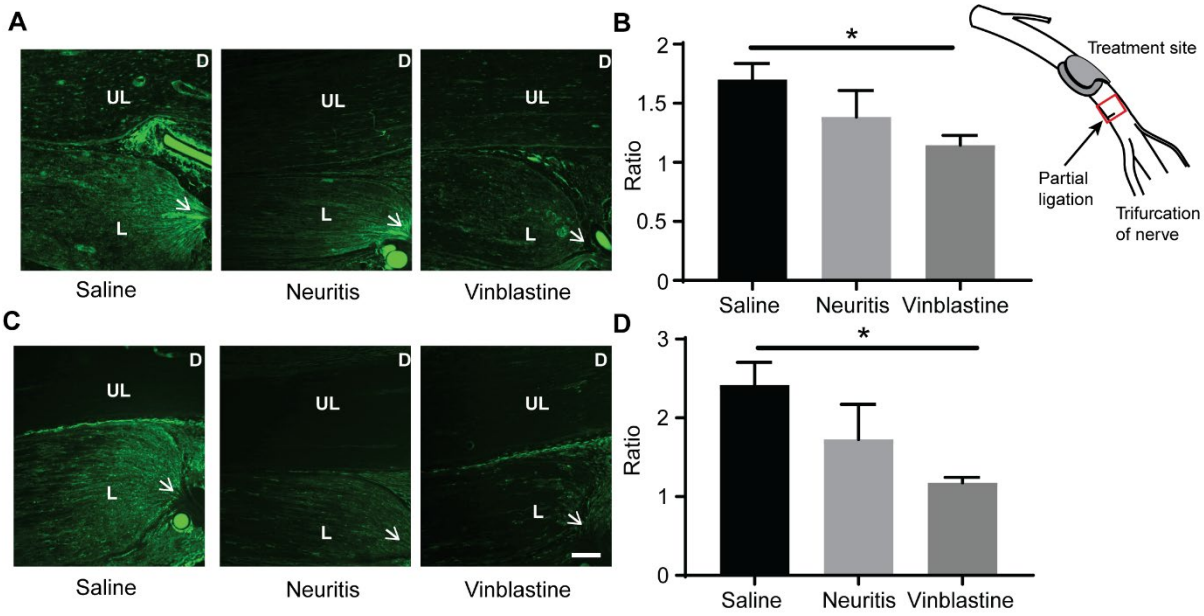

Fig. 4. Axonal transport of TRPV1 and TRPA1. (A) TRPV1 and (C) TRPA1 immunolabeling proximal to the ligation site in saline-treated, neuritis and vinblastine-treated groups. The ligation was immediately distal to the treatment site. (B, D) Mean ratio of TRPV1 immunolabeling (ligated portion / equivalent unligated portion). P = proximal, D = distal, L = ligated portion of the nerve, UL = unligated portion of the nerve. Insert: Methods schematic showing sciatic nerve in the thigh. Note the red box represents the approximate position of the sections. D = distal, L = ligated portion of the nerve, UL = unligated portion of the nerve. Arrow head = Ligation site. * $p<0.05$ (one-way ANOVA followed by Fisher's least significant-difference post hoc test, correcting for the false discovery rate). In B, n = 5, 3, 5 saline-treated, neuritis and vinblastine treated animals respectively. In D, n = 4, 3, 4 saline-treated, neuritis and vinblastine treated animals respectively. Error bars +/- SEM. Scale Bar = 100μM.

Supplementary material

Table. Activity rates of AMS neurons following neuritis and vinblastine treatment, and neurons in an untreated group, at baseline (Pre-drug) and following topical application of 200 μM OLDA or 500 μM cinnamaldehyde (Post-drug).

			Activity rate (Hz), mean (SEM)		p	
Model	**Agent**	**n**	**Pre-**	**Post-**	**Interaction**	**Time**
Neuritis	OLDA	11	0.054 (0.027)	0.052 (0.013)	0.99	0.80
	Cinnamaldehyde		0.065 (0.030)	0.062 (0.021)		
Vinblastine	OLDA	8	0.059 (0.032)	0.110 (0.054)	0.66	0.11
	Cinnamaldehyde		0.098 (0.079)	0.128 (0.072)		
Untreated	OLDA	11	0.034 (0.018)	0.053 (0.022)	0.74	0.06
	Cinnamaldehyde		0.027 (0.014)	0.041 (0.019)		

The mean post-intraneural injection activity rate was calculated from the 2 min bin with the maximum firing rate for each neuron. P values are shown for both the interaction and time (pre- versus post-activity level; two-way ANOVA).